Diagnostic Performance of Cardiac Magnetic Resonance Imaging and Echocardiography in Evaluation of Cardiac and Paracardiac Masses

Rima Patel, MD[a], Ruth P. Lim, MD[b], Muhamed Saric, MD[c], Ambika Nayar, MD[c], James Babb, PhD[d], Mark Ettel, MD[e], Leon Axel, MD, PhD[d], and Monvadi B. Srichai, MD[f,*]

Echocardiography is the preferred initial imaging method for assessment of cardiac masses. Cardiac magnetic resonance (CMR) imaging, with its excellent tissue characterization and wide field of view, may provide additional unique information. We evaluated the predictive value of echocardiography and CMR imaging parameters to identify tumors and malignancy and to provide histopathologic diagnosis of cardiac masses. Fifty patients who underwent CMR evaluation of a cardiac mass with subsequent histopathologic diagnosis were identified. Echocardiography was available in 44 of 50 cases (88%). Echocardiographic and CMR characteristics were evaluated for predictive value in distinguishing tumor versus nontumor and malignant versus nonmalignant lesions using histopathology as the gold standard. The Wilcoxon rank-sum test was used to compare the 2 imaging methods' ability to provide the correct histopathologic diagnosis. Parameters associated with tumor included location outside the right atrium, T2 hyperintensity, and contrast enhancement. Parameters associated with malignancy included location outside the cardiac chambers, nonmobility, pericardial effusion, myocardial invasion, and contrast enhancement. CMR identified 6 masses missed on transthoracic echocardiography (4 of which were outside the heart) and provided significantly more correct histopathologic diagnoses compared to echocardiography (77% vs 43%, p <0.0001). In conclusion, CMR offers the advantage of identifying paracardiac masses and providing crucial information on histopathology of cardiac masses. Published by Elsevier Inc. (Am J Cardiol 2016;117:135−140)

The primary objective of this study was to evaluate the predictive value of echocardiography and cardiac magnetic resonance (CMR) imaging parameters to identify cardiac tumors and malignant masses (Table 1),[1] as well as to diagnose the histopathology for cardiac masses using histologic confirmation as the gold standard. We hypothesized that CMR provides incremental diagnostic value to echocardiography.

Methods

Our study was approved by the institution review board at our medical center in compliance with the Health Insurance Portability and Accountability Act.

We retrospectively identified 171 patients (58% men, age 55 ± 19 years) referred for CMR evaluation of cardiac/paracardiac mass from October 2004 to February 2011. Of these 171 patients, 121 patients were managed conservatively (Figure 1). Six malignant masses were managed conservatively because of poor surgical candidacy, unresectability, and patient preference. Tissue for histopathology was obtained in 50 patients through either percutaneous (n = 7) or surgical (n = 43) approaches after CMR study; 44 had echocardiograms.

Transthoracic echocardiography (TTE) was performed using commercially available equipment (iE33, Sono 7500; Philips Healthcare, Andover, Massachusetts). Images were obtained in standard views. Transesophageal echocardiography (TEE) was also performed using commercially available equipment and standard imaging planes. Contrast agents were not used. Echocardiography studies were clinically interpreted by level 3-trained cardiologists at our institution. TTE was performed in 38 of 44 cases, TEE alone in 6 of 44 cases, and both TTE and TEE in 11 of 44. The reports were reviewed for imaging parameters (see statistical analysis). If a mass was missed on TTE and seen on TEE (as in 1 case), TEE served as the reference point.

CMR studies were performed on a 1.5-T (Avanto or Sonata) or 3.0-T (TimTrio or Verio) MR system (Siemens Healthcare, Erlangen, Germany) using a torso and spine coil in conjunction with electrocardiographic gating. Imaging was performed with standard cardiac mass evaluation protocol consisting of the following sequences in all patients: (1) scout images to identify cardiac axes, (2) black-blood double inversion recovery imaging of the thorax in axial

[a]Department of Cardiology, Mount Sinai Beth Israel Medical Center, New York, New York; [b]Department of Radiology, The Austin Hospital, Heidelberg, Victoria, Australia; [c]Division of Cardiology, Department of Medicine, [d]Department of Radiology, and [e]Department of Pathology, New York University School of Medicine, New York, New York; and [f]Division of Cardiology, Department of Medicine, MedStar Georgetown University Hospital, MedStar Heart Institute, Washington, DC. Manuscript received August 14, 2015; revised manuscript received and accepted October 9, 2015.

This project was supported by grant number K12HS019473 from the Agency for Healthcare Research and Quality (Rockville, Maryland).

See page 140 for disclosure information.

*Corresponding author: Tel: (202) 444-5515; fax: (877) 303-1461.

E-mail address: srichai@alum.mit.edu (M.B. Srichai).

0002-9149/15/$ - see front matter Published by Elsevier Inc.
http://dx.doi.org/10.1016/j.amjcard.2015.10.014

Table 1
World Health Organization 2015 classification of tumors of the heart

Benign tumors and tumor-like lesions
Rhabdomyoma
Histiocytoid cardiomyopathy
Hamartoma of mature cardiac myocytes
Adult cellular rhadomyoma
Cardiac myxoma
Papillary fibroelastoma
Haemangioma, NOS
Capillary Haemangioma
Cavernous Haemangioma
Cardiac fibroma
Lipoma
Cystic tumor of the atrioventricular node
Granular cell tumor
Schwannoma
Tumors of uncertain behavior
Inflammatory myofibroblastic tumor
Paraganglioma
Germ cell tumors
Teratoma, mature
Teratoma, immature
Yolk sac tumor
Malignant Tumors
Angiosarcoma
Undifferentiated pleomorphic sarcoma
Osteosarcoma
Myxofibrosarcoma
Leiomyosarcoma
Rhabdomyosarcoma
Synovial sarcoma
Miscellaneous sarcomas
Cardiac lymphomas
Metastatic tumors
Tumors of the pericardium
Solitary fibrous tumor, malignant and nonmalignant
Angiosarcoma
Synovial sarcoma
Malignant mesothelioma
Germ cell tumors
Teratoma, mature and immature
Mixed germ cell tumor

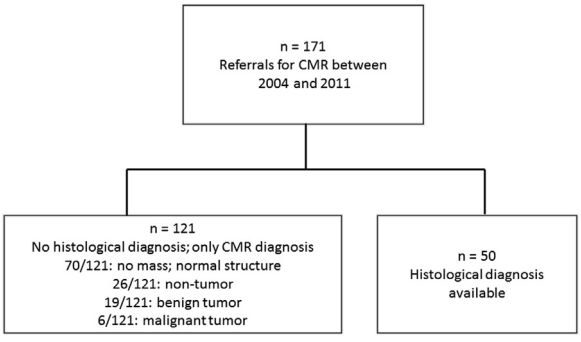

Figure 1. Summary of patients included in cohort.

and sagittal planes, (3) cine 2-dimensional steady-state free precession (SSFP) imaging in stacked horizontal long axis (4-chamber) and short-axis planes to cover the entire heart, (4) T1-weighted and T2-weighted fast turbo spin echo and short tau inversion recovery sequences, (5) dynamic first-pass perfusion after an intravenous injection of 0.15 mmol/kg gadolinium-DTPA, (6) precontrast and post-contrast 3-dimensional volumetric interpolated breath-hold sequence performed in the axial planes, and (7) post-contrast T1-weighted fast turbo spin echo and inversion recovery late gadolinium enhancement imaging (5 to 10 minutes after contrast). CMR studies were clinically interpreted by 1 of 3 level 3 CMR-trained physicians at our institution. The finalized CMR reports were reviewed for information on characteristics of the mass.

Table 2
Patient characteristics including final pathologic diagnosis (n = 50)

	All Patients (*n=50*)	Men (*n=25*)	Women (*n=25*)
Age (mean ± SD)	**46±17**	**46±17**	**46±17**
Previous Cancer History	**10**	**4**	**6**
History of Atrial Fibrillation	**2**	**2**	**0**
History of CVA*	**3**	**1**	**2**
Non-tumor	**15**	**8**	**7**
Thrombus	9	4	5
Mitral valve with myxoid degeneration	2	2	0
Pericardial cyst	1	1	0
Non-neoplastic liver	1	0	1
Thymic cyst	1	0	1
Intramyocardial cyst	1	1	0
Benign Tumor	**14**	**6**	**8**
Myxoma	9	5	4
Papillary fibroelastoma	3	0	3
Lipoma	1	1	0
Lipoleiomyoma	1	0	1
Malignant Tumor	**21**	**11**	**10**
Teratoma	2	0	2
Paraganglioma	2	1	1
Thymoma	2	1	1
Hodgkin's lymphoma	1	1	0
Diffuse large B-cell lymphoma	3	1	2
Non-small cell adenocarcinoma	1	0	1
Metastatic breast cancer	1	0	1
Metastatic clear cell renal cancer	1	0	1
Poorly differentiated sarcoma	1	1	0
Osteosarcoma	1	1	0
Fibrosarcoma	1	1	0
Liposarcoma	2	1	1
Desmoplastic sarcoma	1	1	0
Rhabdomyosarcoma	1	1	0
Angiosarcoma	1	1	0

Bold indicates timing of new category.
* CVA = cerebrovascular accident.

Table 3
Location of masses

Location	Non-Tumor	Benign Tumor	Malignant Tumor
Right Atrium	8	3	5
Right Ventricle	0	2	2
Left Atrium	2	8	0
Left Ventricle	2	0	1
Pericardium	0	0	5
Epicardial	0	0	1
Extracardiac	3	1	8

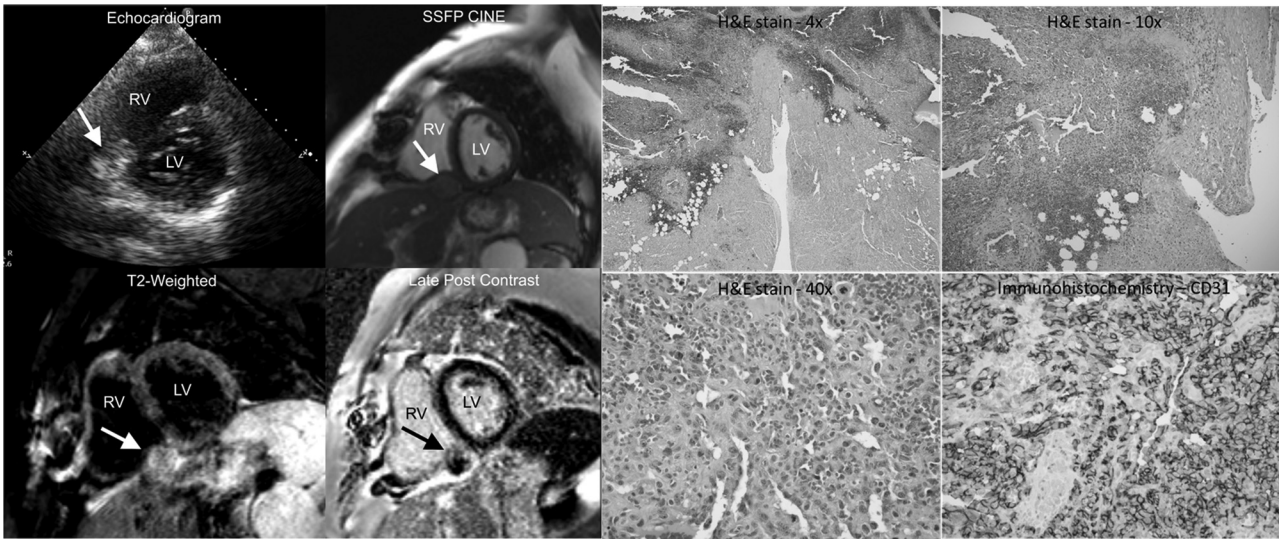

Figure 2. Sixty-eight-year-old man with previously resected cardiac sarcoma with new onset atrial fibrillation. TTE in basal short-axis view retrospectively demonstrates a mass *(arrow)* in the inferior RV, missed on initial evaluation. Cine CMR in short-axis view demonstrates an intrapericardial mass near the inferior RV wall, which is hyperintense to myocardium on T2-weighted images with peripheral contrast enhancement on first-pass and late gadolinium enhancement images. Histopathology demonstrated angiosarcoma. An infiltrative mass with extensive areas of hemorrhage is seen at low power magnification (H&E: 4×) with infiltration into cardiac muscle (H&E: 10×). High power magnification (H&E: 40×) shows slit-like vessels lined by atypical cells with plump irregular nuclei and prominent nucleoli, with multiple mitoses. Tumor cells are reactive for CD31 (a protein expressed in vascular tumors) on immunohistochemistry. LV = left ventricle; H&E = hematoxylin and eosin stain; RV = right ventricle; SSFP = steady-state free precession.

Table 4
Echocardiography and cardiac magnetic resonance imaging parameters predictive of tumor or malignancy

Echocardiography Parameters	Unadjusted		Adjusted for Age and Gender	
	Tumor (*P*-value)	Malignancy (*P*-value)	Tumor (*P*-value)	Malignancy (*P*-value)
Location outside the right atrium	0.0063*	0.4037	0.0049*	0.4661
Location outside the atria and ventricles	0.0405*	0.0054*	0.0444*	0.0044*
Size > 1 cm	0.1351	0.9470	0.1224	0.9137
Non-Mobility	0.5994	0.0031*	0.5084	0.0039*
Number of Masses	0.5165	0.3371	0.5181	0.4324
Myocardial Invasion	0.2300	0.1470	0.3543	0.2233
Pericardial Effusion	0.6863	0.0049*	0.4578	0.0088*
Pleural Effusion	1.0000	0.3864	0.9999	0.3798
Cardiac Magnetic Resonance Parameters	**Tumor (*P*-value)**	**Malignancy (*P*-value)**	**Tumor (*P*-value)**	**Malignancy (*P*-value)**
Location outside the right atrium	0.0145*	0.2002	0.0095*	0.2625
Location outside the atria and ventricles	0.1802	0.0009*	0.1317	0.0015*
Size > 1 cm	0.5404	0.9999	0.4321	0.9999
Non-Mobility	0.5297	0.0009*	0.3740	0.0012*
T1 Hypointensity Pattern	1.0000	0.2053	0.9851	0.2144
T1 Hyperintensity or Mixed Pattern	0.2214	0.9390	0.2565	0.7725
T1 Mixed Pattern	0.9291	0.1074	0.8308	0.1513
T2 Hypointensity Pattern	0.1114	0.0657	0.2321	0.0987
T2 Hyperintensity or Mixed Pattern	0.0099*	0.0855	0.0088*	0.0771
T2 Mixed Pattern	0.4289	0.9605	0.4208	0.9354
Contrast Enhancement on First-Pass	0.0002*	0.0033*	0.0003*	0.0035*
Late Gadolinium Enhancement	<0.0001*	0.0104*	0.0002*	0.0096*
Myocardial Invasion	0.0870	0.0112*	0.1212	0.0345*
Pericardial Effusion	0.1175	0.0035*	0.0710*	0.0047*
Pericardial Involvement	0.6113	0.1040	0.5221	0.1175
Pleural Effusion	0.3414	0.1086	0.2897	0.1290

* p <0.05.

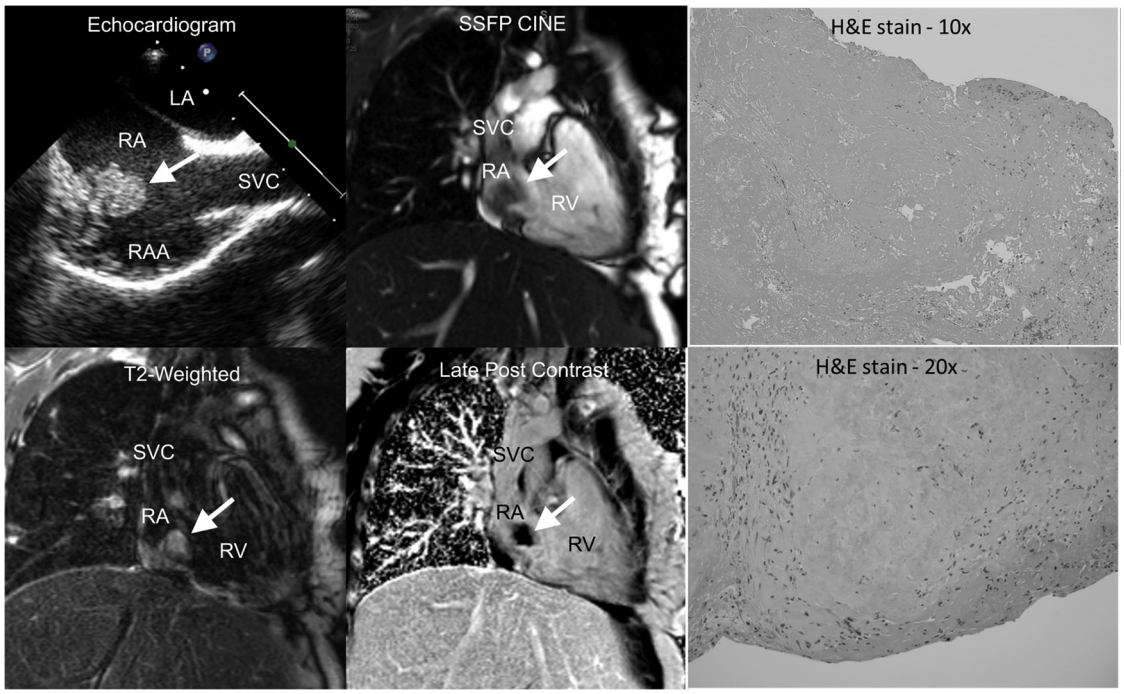

Figure 3. Twenty-year-old woman with sickle cell disease and RA mass. TEE in bicaval view demonstrates an echogenic, mobile mass near the RAA. Cine CMR in right-sided 2-chamber view demonstrates mobile RA mass with increased signal intensity on T2-weighted images and no contrast enhancement. Histopathology demonstrated bland atrial thrombus. The thrombus is primarily composed of fibrin (H&E: 10×) with areas of organization at the periphery of the thrombus (H&E: 20×). The arrow is pointing to the mass. LA = left atrium; RA = right atrial; RAA = right atrial appendage; RV = right ventricle; SVC = superior vena cava.

Continuous data are reported as mean ± SD, and categorical data are expressed as frequency or percentage. Individual morphologic features (location, size, number, mobility, myocardial infiltration, and presence of pericardial or pleural effusion) and imaging characteristics (homogenous/heterogeneous, signal intensity on T1/T2-weighted sequences, and contrast enhancement on first-pass enhancement and late gadolinium enhancement) were evaluated as potentially useful imaging measures for mass diagnosis using binary logistic regression analysis. The Wilcoxon rank-sum test was used to compare the number of times a correct histologic diagnosis was provided by each imaging study using pathology as the reference standard. All statistical tests were conducted at the 2-sided 5% significance level using SAS 9.3 (SAS Institute, Cary, North Carolina).

Results

Fifty patients (50% men, mean age 46 ± 17 years) had histologic diagnosis of their cardiac mass (Table 2). Pathologically confirmed malignant tumors occurred at almost the same frequency in men and women (11 of 25, 44% men vs 10 of 25, 40% women). A total of 10 of 50 patients had a preexisting cancer diagnosis. Of those, 6 of 10 had recurrence of disease on pathology, 2 of 10 had a new primary cancer diagnosis, and 2 of 10 were diagnosed with a thrombus. Location of tumors is listed in Table 3.

In 44 cases (88% of cohort) with echocardiography, CMR was performed after echocardiography at mean interval of 13 ± 34 days. CMR identified a mass lesion in all cases that underwent intervention for histologic diagnosis. CMR was performed 20 ± 34 days before intervention.

In 5 of 44 cases (11%), TTE (TEE not performed) did not identify a mass that was later seen on CMR and pathology. All 5 masses were >3 cm on CMR. Of the missed masses, 2 were in the anterior mediastinum, 2 in the pericardium (Figure 2), and 1 in the left atrium. There was an additional paracardiac mass located in the middle mediastinum that was initially visualized on left heart catheterization, missed on TTE but visualized on TEE.

Table 4 demonstrates individual age-adjusted and gender-adjusted echocardiography and CMR parameters associated with tumor and malignancy.

TTE/TEE provided the correct histopathologic diagnosis in 19 of 44 cases (43%), including 9 of 13 (73%) nonneoplastic masses, and 10 of 14 (71%) benign tumors. Echocardiography did not provide correct pathologic diagnosis for any of the 17 malignant tumors included in our cohort. CMR provided the correct pathologic diagnosis in 34 of 50 cases (68%), including 10 of 15 (67%) nonneoplastic masses, 11 of 14 (79%) benign tumors, and 13 of 21 (62%) malignant tumors. In 44 cases with echocardiography and CMR data, CMR provided significantly more correct pathologic diagnoses compared to echocardiography (77% vs 43%, $p < 0.0001$). All thrombi were correctly identified on CMR. There was 1 case of right atrial papillary fibroelastoma that was correctly diagnosed on echocardiography but misdiagnosed on CMR as myxoma. There were 16 cases that were correctly diagnosed on CMR and not echocardiography, including 3 nontumor masses, 3 benign tumors, and 10 malignant tumors. Representative examples are shown in Figures 2 to 4.

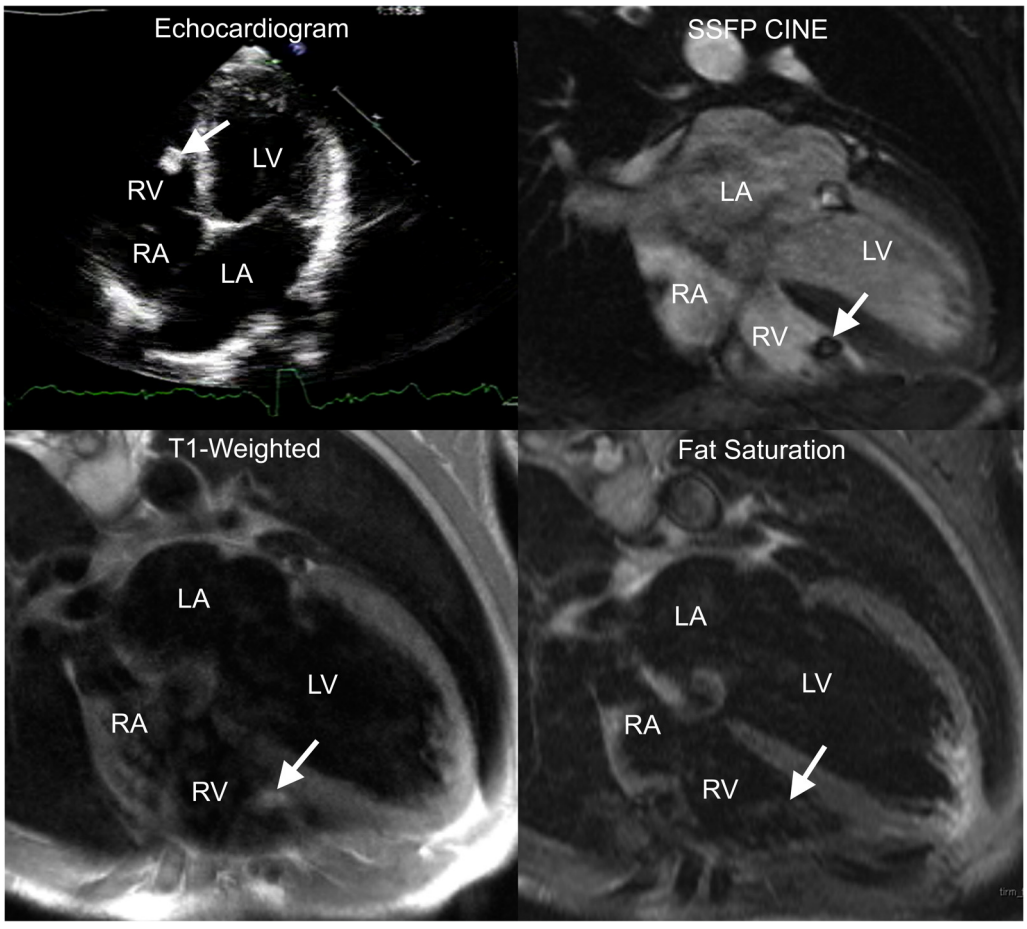

Figure 4. Fifty-year-old man with mitral valve prolapse and flail with an intracardiac mass. TTE in 4-chamber view demonstrates a round, echogenic mass in the right ventricular cavity. Cine CMR shows mobile RV mass attached to the papillary muscle with an increased signal intensity on T1-weighted images which becomes hypointense on fat saturation sequences consistent with a fatty lesion such as lipoma. Histopathology of the mass (not shown) demonstrated lipoma. LA = left atrium; LV = left ventricle; RA = right atrium; RV = right ventricle.

Discussion

There are several important findings in this study. First, we identified echocardiographic and CMR characteristics that were most predictive of cardiac/paracardiac neoplasm, and specifically malignancy. Second, we demonstrated the value of CMR to echocardiography in identifying extracardiac masses. Finally, we found that CMR provided significantly more correct histopathologic diagnosis of a cardiac mass compared to echocardiography alone (77% vs 43%, $p < 0.0001$).

Overall, the data from CMR and echocardiographic imaging parameters and morphologic features (Table 4) we evaluated were consistent with previous reports.[2–4] T2 hyperenhancement was predictive of tumor,[4] likely because of extracellular water content and methemoglobin deposits in tumors from old area of hemorrhage. Contrast enhancement features on CMR (early and late) were predictive of malignancy, likely because of enhancement from tumor vascularity. Morphologic features such as pericardial effusion, immobility, and myocardial invasion helped to distinguish malignant tumors on CMR, whereas immobility on echocardiography was predictive of malignancy. We found that location outside the right atrium was predictive of both tumor and malignancy, which is contradictory to the finding of secondary tumors most commonly metastasizing to the right atrium. The inclusion of paracardiac masses in our cohort may have affected this finding.

TTE is used for assessment of suspected cardiac mass,[5] with sensitivity 93% to 94%.[3,6] Despite high sensitivity, there are several important limitations including detection of extracardiac,[3] left atrial appendage, and right heart masses[7] because of difficulty obtaining these views. TEE offers improved spatial resolution but is less optimal because of its invasiveness. Of 44 cases with echocardiograms, 6 confirmed masses (14%) were missed on TTE. TEE was performed in only 1 of these cases and demonstrated a middle mediastinal mass. The paracardiac location of 5/6 of missed masses on TTE highlights the limitations of TTE in visualizing these masses. All these masses were >3 cm, suggesting that spatial resolution was not a limiting factor in visualization. CMR provided clear value in identifying 100% of the masses missed on initial TTE evaluation altogether. CMR's wide field of view is certainly beneficial in identifying paracardiac masses, which can be easily missed on TTE and TEE.

By nature of its superior tissue characterization, CMR provided significantly more correct histopathologic

diagnoses compared with echocardiography.[4] This was particularly true for malignant masses, none of which received a correct tissue diagnosis with echocardiography. The ability to characterize malignant masses is important for clinical management and prognosis. Not all malignant tumors require surgical resection, and some tumors such as lymphoma are best treated with chemotherapy.[8] Thus, noninvasive imaging techniques that yield further information on pathology may affect downstream clinical management, such as need for surgery versus chemotherapy.

Mass diagnosis using CMR tissue characterization led to misdiagnoses in a few cases in our cohort. A fibroelastoma encased by a thrombus was mistakenly interpreted as a simple thrombus on CMR because of lack of enhancement of the peripheral thrombus with contrast administration (a classic CMR feature of thrombi),[9,10] and a poorly differentiated sarcoma was misdiagnosed as a rapidly spreading infection, again because of lack of enhancement related to rapid central tissue necrosis.

Overall, CMR offers the advantage of identifying paracardiac masses and providing crucial information on histopathology of masses. Results from this study suggest that CMR should be the test of choice in patients with known malignancy with a question of cardiac metastases, as it will provide useful information on histopathology and may identify paracardiac masses missed on echocardiography.

There are several limitations to our study. First, we only evaluated biopsy-proved masses, and therefore, no conservatively managed masses were included. This fact may have influenced the lower prevalence of benign tumors (40%) in our cohort as compared to that quoted in the study of approximately 75%.[11] Second, our data may be biased toward masses undiagnosed on echocardiography as we considered only masses that underwent further evaluation with CMR, and there may have been masses that were definitively diagnosed on echocardiography, obviating the need for additional imaging evaluation. Because it is common practice at our institution for patients to undergo comprehensive imaging evaluation before surgical intervention, this bias is expected to be small. Third, given the heterogeneity of tumors presented and relatively small sample size, significance of specific imaging parameters in distinguishing malignant and benign tumors may have been underestimated because of insufficient powering. Finally, we do not account for interreader variability in our analysis.

Disclosures

The authors have no conflicts of interest to disclose.

1. Travis WD, Brambilla E, Burke AP, Marx A, Nicholson AG. WHO Classification of Tumours of Lung, Pleura, Thymus, and Heart. 4th Edition. Lyon: IARC, 2015:300.
2. Hoffman U, Globits S, Schima W, Loewe C, Puig S, Oberhuber G, Frank H. Usefulness of magnetic resonance imaging of cardiac and paracardiac masses. *Am J Cardiol* 2003;92:890−895.
3. Meng Q, Lai H, Lima J, Tong W, Qian Y, Lai S. Echocardiographic and pathologic characteristics of primary cardiac tumors: a study of 149 cases. *Int J Cardiol* 2002;84:69−75.
4. Pazos-Lopez P, Pozo E, Siqueira ME, Garcia-Lunar I, Cham M, Jacobi A, Macaluso F, Fuster V, Narula J, Sanz J. Value of CMR for the differential diagnosis of cardiac masses. *JACC Cardiovasc Imaging* 2014;7:896−905.
5. Douglas PS, Garcia MJ, Haines DE, Lai WW, Manning WJ, Patel AR, Picard MH, Polk DM, Ragosta M, Ward RP, Weiner RB. ACCF/ASE/AHA/ASNC/HFSA/HRS/SCAI/SCCM/SCCT/SCMR 2011 Appropriate Use Criteria for Echocardiography: a report of the American College of Cardiology Foundation Appropriate Use Criteria Task Force, American Society of Echocardiography, American Heart Association, American Society of Nuclear Cardiology, Heart Failure Society of America, Heart Rhythm Society, Society for Cardiovascular Angiography and Interventions, Society of Critical Care Medicine, Society of Cardiovascular Computed Tomography, and Society for Cardiovascular Magnetic Resonance Endorsed by the American College of Chest Physicians. *J Am Soc Echocardiogr* 2011;24:229−267.
6. Fyke FE 3rd, Seqard JB, Edwards WD, Miller FA Jr, Reeder GS, Schattenberg TT, Schub C, Callahan JA, Tajik AJ. Primary cardiac tumors: experience with 30 consecutive patients since the introduction of two-dimensional echocardiography. *J Am Coll Cardiol* 1985;5:1465−1473.
7. Mugge A, Daniel WG, Haverich A, Lichtlen PR. Diagnosis of noninfective cardiac mass lesions by two-dimensional echocardiography. Comparison of the transthoracic and transesophageal approaches. *Circulation* 1991;83:70−78.
8. Evans LS, Hancock BW. Non-Hodgkin lymphoma. *Lancet* 2003;362:139−146.
9. Mollet NR, Dymarkowski S, Volders W, Wathiong J, Herbots L, Rademakers FE, Bogaert J. Visualization of ventricular thrombi with contrast-enhanced magnetic resonance imaging in patients with ischemic heart disease. *Circulation* 2002;106:2873−2876.
10. Srichai MB, Junor C, Rodriguez L, Stillman AE, Grimm RA, Lieber ML, Weaver JA, Smedira NG, White RD. Clinical, imaging, and pathological characteristics of left ventricular thrombus: a comparison of contrast-enhanced magnetic resonance imaging, transthoracic echocardiography, and transesophageal echocardiography with surgical or pathological validation. *Am Heart J* 2006;152:75−84.
11. McManus B. Primary tumors of the heart. In: Bonow RO, Mann DL, Zipes DP, Libby P, eds. Braunwald's Heart Disease: A Textbook of Cardiovascular Medicine. Philadelphia: Saunders, 2012:1638−1650.